Aerosol light absorption from optical measurements of PTFE-membrane filter samples: sensitivity analysis of optical depth measures

Apoorva Pandey[1], Nishit J. Shetty[1], and Rajan K. Chakrabarty[1,2]

[1]Center for Aerosol Science and Engineering, Department of Energy, Environmental and Chemical Engineering, Washington University in St. Louis, St. Louis, MO 63130, USA
[2]McDonnell Center for the Space Sciences, Washington University in St. Louis, St. Louis, MO 63130, USA

Correspondence to: Rajan K. Chakrabarty (chakrabarty@wustl.edu)

Abstract. Mass absorption cross-section (MAC) measurements of atmospherically-relevant aerosols are required to quantify their effect on Earth's radiative budget. Estimating aerosol light absorption from transmittance and/or reflectance measurements through filter deposits is an attractive option because of ease of deployment in field settings, low cost, and the ability to revisit previously analysed samples. These measurements suffer from artifacts that depend on a given filter measurement system and type of aerosol. Empirical correction algorithms are available for commercial instruments equipped with optically-thick fiber filters, but optically-thin filter media have not been characterized in detail. Here, we present empirical relationships between particle light absorption optical depth–measured using multi-wavelength integrated photoacoustic spectrometers and nephelometers–and filter optical depth measurements for polytetrafluoroethylene (PTFE) membrane filter samples of carbonaceous aerosols generated from combustion of diverse biomass fuels and kerosene (surrogate for fossil-fuel combustion). Through radiative transfer modeling, we assessed the suitability of three measures of optical depth for robustly describing particulate-phase light absorption over a range of single scattering albedo (SSA) values: (1) OD_s–a measure of transmission of the fraction of incident radiation that is not backscattered by the filter system–utilizes reflectance of the sample side of the filter, (2) the commonly-used OD_c uses the reflectance of the clean side of the filter, and (3) ATN or the Beer-Lambert attenuation. Modeling results were also experimentally validated, with OD_s showing the least variability around the mean in this multi-dimensional parameter space. We establish a simple, wavelength-independent formulation for calculating aerosol MAC and absorption coefficients from measurements of OD_s. We find the ratio between in-situ particulate absorption optical depth and OD_s to be inversely proportional to aerosol SSA. Our findings underscore that OD_s is a better optical depth measure than OD_c for applying appropriate correction factors when estimating particle phase light absorption from filter-based techniques.

1 Introduction

Aerosol light absorption affects the radiative balance of the Earth's atmosphere through direct and indirect mechanisms (Bond et al., 2013; Kanakidou et al., 2005; Ramanathan et al., 2001). The light absorption metric relevant to climate modelers–mass absorption cross-section (MAC)–depends on the size, shape and composition of the aerosols (Andreae and

Gelencsér, 2006; Bond and Bergstrom, 2006; Moosmüller et al., 2009). This property has a complex dependency on the emission source, especially for carbonaceous aerosols (Andreae and Gelencsér, 2006; Bond and Bergstrom, 2006; Chakrabarty et al., 2010). The canonical MAC value for "pure" black carbon aerosols, associated with fossil fuel emissions, is 7.5 m^2g^{-1} at 550 nm (Bond et al., 2013). MAC values for absorbing organic carbon, typically released from biomass burning, strongly vary with combustion phase, and can range ~0.01-1 m^2g^{-1} at 550 nm (Laskin et al., 2015).

A first-principle method of measuring contact-free aerosol light absorption is using photoacoustic spectroscopy, which employs lasers at selected wavelengths to heat the aerosols, thereby producing a detectable pressure signal (Arnott et al., 1999). Absorption can also be estimated as the difference between *in-situ* measurements of extinction and scattering (Schnaiter et al., 2005; Sheridan et al., 2005). Alternatively, a commonly adopted technique for estimating light absorption uses measurements of transmittance and/or reflectance for aerosol particles collected on a filter substrate. Instruments developed based on this technique, including the aethalometer (Hansen et al., 1984) and the Particle Soot Absorption Photometer or PSAP (Virkkula et al., 2005), facilitate semi-continuous sampling of particles and produce time-averaged bulk absorption measurements. Particles may also be collected on quartz fiber or Teflon filters and analyzed for their absorption using standalone spectrophotometers (Martins et al., 2009; Pandey et al., 2016; White et al., 2016; Zhong and Jang, 2011).

Filter-based measurements are attractive because of their ease of deployment in field settings and low cost, but they suffer from several artifacts. Particles embedded in a multiple-scattering medium experience a larger optical path length than particles in their native suspended state, leading to the appearance of enhanced light absorption (Bond et al., 1999; Clarke, 1982; Gorbunov et al., 2002). This is referred to the as the multiple scattering artifact, and it depends on the choice of filter medium. A higher loading of absorbing aerosols can diminish the effect of multiple scattering, inducing an aerosol dependent loading artifact (Arnott et al., 2005; Weingartner et al., 2003). Highly scattering aerosols could enhance multiple scattering and lead to increased backscatter, which leads to an overestimation of absorption (Lack et al., 2008; Weingartner et al., 2003). These artifacts have been evaluated for several commonly used filter-based instruments, such as those aforementioned, by comparing their measurements with contact-free aerosol light absorption measurements or using reference materials with known optical properties. Typically, correction algorithms for these artifacts are formulated as functions of some combination of filter and aerosol properties (Arnott et al., 2005; Collaud Coen et al., 2010; Virkkula, 2010; Weingartner et al., 2003) and are specific to a given measurement system.

In various field settings, aerosol samples are collected on polytetrafluoroethylene (PTFE) membrane filters (commonly known as Teflon filters) for inferring ambient or near-source particulate mass concentrations using gravimetric analysis (Koistinen et al., 1999). Major aerosol monitoring networks, such as the Interagency Monitoring of PROtected Visual Environments (IMPROVE) network (Chow et al., 2010; Solomon et al., 2014), the Chemical Speciation Network (CSN) (Solomon et al., 2014) and the Surface PARTiculate mAtter Network (SPARTAN) (Snider et al., 2015), collect particle samples on Teflon filters for gravimetric and elemental measurements. PTFE filters are chemically inert and unlike quartz fiber filters, present a very low surface area for organic vapor adsorption (Kirchstetter et al., 2001; Vecchi et al., 2014).

Correction schemes developed for instruments that use fiber filters (like the PSAP and aethalometer) cannot be applied to infer aerosol light absorption properties using measurements of transmittance and/or reflectance on PTFE filters. A previous study on the artifacts associated with this estimation used a reference material and provided a constant multiple scattering correction factor for optical loadings smaller than a certain threshold (Zhong and Jang, 2011). Another recent study (White et al., 2016) proposed a theory-based model to calibrate attenuation measurements for Teflon filter samples and applied this new model to a historical dataset from IMPROVE network. They found that the reevaluated absorption values for the PTFE samples were well-correlated with thermo-optical elemental carbon (EC) measurements for co-located quartz fiber filters.

In this work, we generated carbonaceous aerosols with varying physicochemical properties from the combustion of biomass fuels and kerosene. Combustion conditions were varied to yield a range of intrinsic aerosol optical properties. Kerosene combustion was used as a surrogate for fossil fuel burning, which is linked with soot or EC emissions (Andreae and Gelencsér, 2006; Bond et al., 2013). The combustion of wildland- and fuel-biomass is implicated in emissions of EC as well as light absorbing organic carbon (LAOC) (Andreae and Gelencsér, 2006; Chakrabarty et al., 2010; Chen and Bond, 2010). EC is known to absorb light throughout the visible and UV wavelengths, while LAOC absorbs preferentially in the near-UV and UV regions (Andreae and Gelencsér, 2006; Bond and Bergstrom, 2006; Kirchstetter et al., 2004; Sun et al., 2007). Therefore, we measured *in-situ* and contact-free aerosol light absorption and scattering coefficients using integrated photoacoustic-nephelometer (IPN) spectrometers operated at three wavelengths - 375, 405 and 532 nm. Co-located with these measurements was a sampling system to collect particles onto Teflon membrane filters. Subsequent filter optical measurements, using ultraviolet-visible (UV-vis) spectrophotometer, were performed. Observed empirical relationships between particle light absorption and filter optical depth were established in conjunction with predictions from a one-dimensional (1-D) two-stream radiation transfer model.

2 Methods

2.1 Two-stream radiative transfer model

A 1-D two-stream radiative transfer framework for multiple scattering in absorbing media was developed in Bohren (1987)–widely known as the Kubelka-Munk theory (Kubelka, 1948)–and subsequently discussed in relation to aerosol-filter systems in several studies (Arnott et al., 2005; Clarke, 1982; Gorbunov et al., 2002; Petzold and Schönlinner, 2004). Solving a radiation balance for an aerosol-laden filter medium yields the following expressions for transmittance (T_l) and reflectance (R_l), respectively:

$$T_l = \frac{2}{[2K - \omega_l(1-g_l)\sinh(K\tau_{e,l}) + 2K\cosh(K\tau_{e,l})]} \tag{1A}$$

$$R_l = \frac{\omega_l(1-g_l)\sinh(K\tau_{e,l})}{[2K - \omega_l(1-g_l)\sinh(K\tau_{e,l}) + 2K\cosh(K\tau_{e,l})]} \tag{1B}$$

Here, ω_l, g_l and $\tau_{e,l}$ denote the single scattering albedo (SSA), asymmetry parameter and extinction optical depth, respectively, of the composite layer. The parameter K is defined as:

$$K = \sqrt{(1-\omega_l)(1-g_l\omega_l)} \tag{2}$$

Arnott et al. (2005) used the above model to derive the form for an approximate correction factor for the aethalometer. The aethalometer uses optically-thick quartz fiber filters, which are strongly multiple scattering, transmitting only ~10% of light in the visible wavelengths. A mathematical consequence of strong multiple scattering is that the term $K\tau_{e,l}$ is much greater than unity and Eq.s (4A) and (4B) can be replaced by simplified approximations. In contrast, the Teflon filters used in this study are optically thin and constitute a weak multiple scattering medium: they transmit 70-80% of incident visible light. Therefore, the full equations for T_l and R_l were solved for the filter-particle system, using a range of plausible values of dimensionless aerosol optical properties: absorption optical depth ($\tau_{a,s}$) and SSA. Two other required inputs could not be measured: the penetration depth of aerosols into the filter was assumed to be 10%, and the asymmetry parameter of the aerosols was fixed at 0.6, based on the typical values reported for biomass burning emissions (Martins et al., 1998; Reid et al., 2005). A schematic representation of the two-layer system–the aerosol laden layer with properties T_l and R_l and a clean filter layer with properties T_f and R_f–is shown in Fig. 1. Transmittance and reflectance (T_s and R_s, respectively) through the filter, when light is first incident on the aerosol-laden layer is given by (Gorbunov et al., 2002):

$$T_s = \frac{T_l T_f}{1 - R_l R_f} \tag{3A}$$

$$R_s = R_l + \frac{T_l^2 R_f}{1 - R_l R_f} \tag{3B}$$

If the light first passes through the clean filter layer, the model predicts that transmittance, T_c, is still given by Eq. (6A). However, filter substrates are not uniform over their depths and have visually distinguishable front and back surfaces. Therefore, measurements of T_s and T_c are expected to differ. For the model substrate, reflectance is given by:

$$R_c = R_f + \frac{T_f^2 R_l}{1 - R_l R_f} \tag{4}$$

Attenuation (ATN) due to the aerosol deposit is calculated by applying Beer-Lambert's law relating to the reduction in transmittance of an exposed filter (T_s) relative to a blank (T_b) (Bond et al., 1999; Campbell et al., 1995). For a non-absorbing filter substrate, all attenuation of incident light must be caused by aerosol light absorption. Therefore, ATN is a measure of $\tau_{a,s}$.

$$ATN = \ln\left(\frac{T_b}{T_s}\right) = \ln\left(\frac{1-R_b}{T_s}\right) \tag{5}$$

Here, R_b is the reflectance of the blank. An alternate measure of filter-aerosol optical depth utilizes transmittance and reflectance of the clean face of the filter (Campbell et al., 1995; White et al., 2016), which can be assumed to be

approximately equal to R_b. The numerator in Eq. (8) can then be replaced by $T_b = 1 - R_b \approx 1 - R_c$. It should be noted that for translucent Teflon filters, R_b and R_c cannot be assumed to be exactly equal (Campbell et al., 1995; Clarke, 1982). Therefore, we represent this measure of optical depth by a separate variable, OD_c, where the subscript denotes that the transmittance and reflectance values used corresponds to the clean side of the filter:

5   $$OD_c = \ln(\frac{1-R_c}{T_c}) \tag{6}$$

Finally, we define an optical depth measure using sample-side transmittance and reflectance, which can be interpreted as a measure of transmission of the fraction of incident radiation that is not backscattered by the filter-aerosol system:

$$OD_s = \ln(\frac{1-R_s}{T_s}) \tag{7}$$

Values of ATN, OD_c and OD_s for a range of $\tau_{a,s}$ values (0-1) are shown in Fig. 2 for two cases: (1) highly absorbing aerosols
10 (SSA=0.3) and (2) highly scattering aerosols (SSA=0.95). We illustrate that OD_c is nearly equal to ATN for the absorbing aerosol case, but there are significant differences between the two optical measures when the filter is loaded with highly scattering aerosols. This is because a translucent substrate with a reflective coating on its back behaves like a mirror: reflectance of the substrate increases when such a coating is applied. We also find that ATN shows the largest variation with SSA for a given value of $\tau_{a,s}$ while OD_s exhibits the smallest variation. This can be attributed to the changing relationships
15 between R_s and filter loading for different SSA values (see Supplement Fig. S2). For large SSA, $R_s>R_b$ and therefore, from Eq.s (5) and (7), $OD_s<ATN$. The converse is true for small SSA values. It should be noted that fixed blank optics–based on the mean of transmittance and reflectance measurements (measurement techniques are described in the following section) on
20 blank filters–were used to model ATN, OD_c and OD_s. The purpose of this exercise was to illustrate the sensitivity of the above optical depth measures to SSA values of aerosols deposited on identical media.

20 The variation in filter optical measures with SSA was quantified by calculating the means and standard deviations of ATN, OD_c and OD_s, over SSA values ranging 0.2-0.99 for each input value of $\tau_{a,s}$. A total of 500 linearly spaced points along the SSA range were used. Blank filter properties were also varied within the model in accordance with the range observed over the 20 lab blanks. For every model sample, defined by a given SSA and $\tau_{a,s}$ combination, a model blank was generated from a normal distribution of blank transmittance (mean=0.7, standard deviation = 0.02). Fig. 3 shows the ratio of standard
25 deviation to the corresponding average values of each filter optical depth measure. The relatively low standard deviation in OD_s (for most loading values) implies that this variable is a good candidate for estimating aerosol light absorption from filter optical measurements, for a wide range of aerosol types. The increase in standard deviation with increasing loading is mainly contributed by very high SSA points which are typically associated with lower absorption per unit mass: therefore very high mass loadings of such aerosols would be required to yield the upper range of the $\tau_{a,s}$. For SSA<0.9, modeled attenuation
30 values show little spread (<15% variability around the mean) with changing SSA. A surface plot of OD_s for all model data points (0.2<SSA<0.99 and 0<$\tau_{a,s}$<1) is shown in the Supplement Fig. S4.

2.2 Experiments

Diverse biomass fuels including wood and needles from pine, fir and sage trees, grass, peat and cattle dung were burned in a 21 m^3 stainless steel combustion chamber located at Washington University Sumlin et al. (2018); Sumlin et al. (2017). Flaming, smoldering and mixed combustion phases were employed (see Supplement) to generate a range of intrinsic aerosol

5 properties: SSA values at 375, 405 and 532 nm ranged 0.25-0.99 and Absorption Ångström Exponents (AÅE) for 375-532 nm ranged 1.2-6.8. A kerosene lamp was used to generate soot particles, with an SSA of 0.3 and AÅE within 0.70-1.1. A schematic of the experimental setup is shown in Fig. 4. Experimental conditions and intrinsic aerosol optical properties are listed in Table 1. Approximately 10-50 g of a given type of woody biomass/grass/dung was placed in a stainless-steel pan and ignited using a flame. It was either allowed to continue flaming or brought to a smoldering phase by starving the flame

10 with a lid. In the same type of pan, 5-15 g of peat was smoldered by using a ring heater to raise its temperature to 200 ⁰C. In one set of experiments, smoke from the chamber was directly sampled, while in another set, a hood placed over the pan was used for sampling the aerosols. The chamber exhaust was closed during the burns. The outlet from the hood or chamber was passed through a diffusion dryer and a semi-volatile organic compound (SVOC) denuder into a mixing volume, from which aerosols were continuously sampled by the four IPNs.

During each burn, optical (absorption and scattering coefficients) signals were monitored using IPNs until a steady state was reached. During the steady state, particle samples were collected on 47 mm PTFE membrane (Pall) filters. The filter sampling flow rate was set to 5 liters per minute and the sampling durations were between 2 and 20 minutes. For each filter sample, $\tau_{a,s}$ of the deposited aerosols was calculated from the absorption coefficients measured using the IPNs:

20 $$\tau_{a,s} = \frac{b_{abs,av} \times Q \times t_s}{10^9 A_s}$$ (8)

where $b_{abs,av}$ is the average absorption coefficient (in Mm^{-1}) during the sampling duration t_s (in min), Q is the flow rate (in liters per minute or lpm) through the filter and A_s is the filter sample area (in m^2). Optical depth $\tau_{a,s}$ for the samples in this study ranged between 0.01 and 0.68. The uncertainty in these estimates was predominantly from the standard deviation in $b_{abs,av}$ over the averaging interval, and was within 10% for all samples. Values of $b_{abs,av}$ at 532 nm ranged from ~300 Mm^{-1}

25 for smoldering samples to ~20000 Mm^{-1} for flaming phase samples; the corresponding range at 375 nm was ~3000-30000 Mm^{-1}.

Transmittance (T_s) and reflectance (R_s) for the filter samples were measured using a Perkin-Elmer LAMBDA 35 UV-vis spectrophotometer (described in Zhong and Jang (2011)). This instrument contains an integrating sphere and two sample holders. Transmittance was measured by placing the sample in the first holder ahead of the sphere, in the direction of the

30 sample beam, while a white standard was placed in the second holder (behind the sphere). Reflectance was measured by keeping the first holder empty and placing the sample in the second holder. Both measurements were performed on the sample face of the filter: light was incident on the face that was exposed to the sample air. Each measurement was

normalized to the baseline value of the measurement system: between every 10 sample scans, transmittance/reflectance were measured with no sample placed in the first holder and a white standard was placed in the second holder. Sample transmittance/reflectance were then divided by the corresponding baseline. Only T_s and R_s were measured for all samples in this study as model results indicated that OD_s is better suited than OD_c for estimating $\tau_{a,s}$ (Fig. 3). To test the validity of this assumption, transmittance and reflectance were also measured on the clean side of the filter (T_c and R_c, respectively) for a subset of the samples (n=54). This subset corresponded to samples collected during 17 biomass burning experiments which yielded aerosols with SSA (375, 405 and 532 nm) ranging 0.54-0.99. For all samples, we found $T_s > T_c$.

From normalized T_s and R_s measurements, OD_s was calculated using Eq. (7). When this equation is applied to blank filters, it results in OD_s values between 0.01-0.03. A wavelength dependent "blank optical depth" was subtracted from the sample attenuation values. Triplicate transmission and reflection measurements were used to estimate measurement uncertainty, which is attributable to random fluctuations in the measurements. Means and standard deviations of the OD_s values calculated from the replicate measurements yielded an uncertainty (ratio of standard deviation to mean) of 5% in OD_s. Similarly, OD_c was calculated for the 54-sample subset.

A correction factor (C) that captures the net effect of multiple scattering and aerosol loading can be defined as:

$$\tau_{a,s} = C \times OD_s \implies C = \frac{\tau_{a,s}}{OD_s} \tag{9}$$

3 Results and discussion

Modeled and experimental values of OD_s for the filter samples are shown in Fig. 5. The two datasets are highly correlated (Pearson R= 0.92), but the model predicted larger values of OD_s than those experimentally determined. This disagreement may partially be due to differences between assumed parameters in our model and their deviation from real-world values. It is also possible that assuming an average propagation direction of diffuse radiation within the two-stream approximation (Arnott et al., 2005; Sagan and Pollack, 1967) causes this systematic difference.

In Fig. 6, we combined all experimental ($\tau_{a,s}$ versus OD_s) data corresponding to the three wavelengths since our measurements showed no clear stratification with varying wavelength. The relationships between $\tau_{a,s}$ and modeled values of OD_s, OD_c and ATN are presented in the Supplement; modelling predicts the lowest scatter in the $\tau_{a,s}$-OD_s curve (Fig. S5). Further, Fig. 7 shows $\tau_{a,s}$ plotted against measured OD_s and OD_c (at all three wavelengths) for the aforementioned 54 filter sample subset, demonstrating that $\tau_{a,s}$ is better correlated with OD_s than with OD_c. Ordinary least-squares regression was applied to obtain power-law fits included in the plot legend. The corresponding relationship for all points in Fig. 6 is given by (R^2 = 0.87):

$$\tau_{a,s} = 0.48 \, (OD_s)^{1.32} \tag{10}$$

Also shown in the figure are estimated $\tau_{a,s}$ using a constant correction factor C of 0.67 proposed by Zhong and Jang (2011) (black perforated line); this correction factor clearly overestimates $\tau_{a,s}$ for most OD_s values investigated in this study. We

find our data to be better represented by an approximate $C = 0.46$ based on a linear least-squares fit ($R^2 = 0.79$). However, any constant C value does not capture the non-linearity of the interaction between aerosol properties and the multiple-scattering within the filter medium. It should be noted that C in Eq. (3) represents the net effects of all filter artifacts. There are measurement errors associated with both OD_s and $\tau_{a,s}$, and therefore, C contains propagation of uncertainties from both

5   parameters. There was no correlation between C and OD_s (see Fig. S6). We observed an inverse relationship between C and SSA (Fig. 8), consistent with results the from the two-stream radiative transfer model. For a given value of $\tau_{a,s}$, measured OD_s will always be higher for aerosols with higher SSA values. Consequently, we should expect C to decrease with increasing SSA; this decreasing relationship for our experimental data is given by:

$$C = -0.76 * SSA + 1.02 \qquad (11)$$

10   Values of C and SSA for individual samples (shown in supplemental Fig. S7B) were aggregated into five SSA bins to demonstrate the inapplicability of an empirical correction factor formulation to low SSA data points in this study. The large spread in C values for low SSA is likely due to noise amplification from dividing two small ($\tau_{a,s}$ and $OD_s < 0.2$) numbers. For SSA>0.6, the correction factor decreases linearly.

5 Summary

15   We evaluated the relationship between *in-situ* aerosol light absorption and attenuation of aerosol deposits on Teflon filters for combustion aerosols (encompassing $0.25 \leq SSA \leq 0.99$), at 375, 405 and 532 nm wavelengths. An empirical non-linear relationship was found between the absorption optical depth of sampled aerosols and attenuation through filter samples; the nature of this function was consistent with predictions from a two-stream radiative transfer model of the filter-aerosol system. Following Eq. (10), we propose the estimation of Aerosol MAC (m^2g^{-1}) values from filter OD_s measurements using:

20    $$MAC = [0.48 \, (OD_s)^{1.32}]\frac{A_s}{m} \qquad (12)$$

where A_s is the filter sample area (in m^2) and m is the mass on deposited particles (in g). Additionally, aerosol absorption coefficients (b_{abs}; in Mm^{-1}) can also be calculated using:

$$b_{abs} = [0.48 \, (OD_s)^{1.32}]\frac{10^9 A_s}{Q \times t_s} \qquad (13)$$

The quantities Q and t_s are as used in Eq. (8). Caution must be taken, as suggested by the two-stream model results, on the
25   limits of applicability of the empirical relationships (equations 10-13)–significant errors could result from application of the relationships if the aerosol SSA>0.9 and OD_s values are beyond the range of this work.

Teflon filters are routinely used for gravimetric and elemental analysis across monitoring networks (Chow et al., 2010; Snider et al., 2015; Solomon et al., 2014), as well as field and laboratory source characterization studies. In many measurement systems, such as the Hybrid Integrating Plate and Sphere (HIPS) method (Bond et al., 1999) used by the
30   IMPROVE network, transmittance and reflectance are measured on the clean side of the filter and the optical depth OD_c is

calculated (Campbell et al., 1995; White et al., 2016). The relationship between aerosol optical depth, $\tau_{a,s}$, and OD_c showed a larger variability across varying SSA than that between $\tau_{a,s}$ and OD_s. Therefore, we suggest further evaluation of OD_s as an optical depth measure that can be empirically connected to particulate phase light absorption for a range of aerosol types.

5 Supplement

Includes a schematic of the experimental setup (Text S1), detailed equations for the two-stream model (Text S2, Figure S1), supplemental modeling results (Text S2, Figures S2-S5), and correction factor plots (Text S3, Figure S6).

Acknowledgements

This work was partially supported by the National Science Foundation under Grant No. AGS1455215, NASA ROSES under Grant No. NNX15AI66G, and the International Center for Energy, Environment and Sustainability (InCEES) at Washington University in St. Louis.

References

Andreae, M. and Gelencsér, A.: Black carbon or brown carbon? The nature of light-absorbing carbonaceous aerosols, Atmospheric Chemistry and Physics, 6, 3131-3148, 2006.

Arnott, W. P., Hamasha, K., Moosmüller, H., Sheridan, P. J., and Ogren, J. A.: Towards aerosol light-absorption measurements with a 7-wavelength aethalometer: Evaluation with a photoacoustic instrument and 3-wavelength nephelometer, Aerosol Science and Technology, 39, 17-29, 2005.

Arnott, W. P., Moosmüller, H., Rogers, C. F., Jin, T., and Bruch, R.: Photoacoustic spectrometer for measuring light absorption by aerosol: instrument description, Atmos. Environ., 33, 2845-2852, 1999.

Bohren, C. F.: Multiple scattering of light and some of its observable consequences, Am. J. Phys, 55, 524-533, 1987.

Bond, T. C., Anderson, T. L., and Campbell, D.: Calibration and intercomparison of filter-based measurements of visible light absorption by aerosols, Aerosol Science & Technology, 30, 582-600, 1999.

Bond, T. C. and Bergstrom, R. W.: Light absorption by carbonaceous particles: An investigative review, Aerosol science and technology, 40, 27-67, 2006.

Bond, T. C., Doherty, S. J., Fahey, D., Forster, P., Berntsen, T., DeAngelo, B., Flanner, M., Ghan, S., Kärcher, B., and Koch, D.: Bounding the role of black carbon in the climate system: A scientific assessment, Journal of Geophysical Research: Atmospheres, 118, 5380-5552, 2013.

Campbell, D., Copeland, S., and Cahill, T.: Measurement of aerosol absorption coefficient from Teflon filters using integrating plate and integrating sphere techniques, Aerosol science and technology, 22, 287-292, 1995.

Chakrabarty, R., Moosmüller, H., Chen, L.-W., Lewis, K., Arnott, W., Mazzoleni, C., Dubey, M., Wold, C., Hao, W., and Kreidenweis, S.: Brown carbon in tar balls from smoldering biomass combustion, Atmospheric Chemistry and Physics, 10, 6363-6370, 2010.

Chen, Y. and Bond, T.: Light absorption by organic carbon from wood combustion, Atmospheric Chemistry and Physics, 10, 1773-1787, 2010.

Chow, J. C., Watson, J. G., Green, M. C., and Frank, N. H.: Filter light attenuation as a surrogate for elemental carbon, J. Air Waste Manage. Assoc., 60, 1365-1375, 2010.

Clarke, A. D.: Effects of filter internal reflection coefficient on light absorption measurements made using the integrating plate method, Applied optics, 21, 3021-3031, 1982.

Collaud Coen, M., Weingartner, E., Apituley, A., Ceburnis, D., Fierz-Schmidhauser, R., Flentje, H., Henzing, J., Jennings, S. G., Moerman, M., and Petzold, A.: Minimizing light absorption measurement artifacts of the Aethalometer: evaluation of five correction algorithms, Atmos. Meas. Tech., 3, 457-474, 2010.

Gorbunov, B., Hamilton, R., and Hitzenberger, R.: Modeling radiative transfer by aerosol particles on a filter, Aerosol Sci. Technol., 36, 123-135, 2002.

Hansen, A., Rosen, H., and Novakov, T.: The aethalometer—an instrument for the real-time measurement of optical absorption by aerosol particles, Sci. Total Environ., 36, 191-196, 1984.

Kanakidou, M., Seinfeld, J., Pandis, S., Barnes, I., Dentener, F., Facchini, M., Dingenen, R. V., Ervens, B., Nenes, A., and Nielsen, C.: Organic aerosol and global climate modelling: a review, Atmospheric Chemistry and Physics, 5, 1053-1123, 2005.

Kirchstetter, T. W., Corrigan, C. E., and Novakov, T.: Laboratory and field investigation of the adsorption of gaseous organic compounds onto quartz filters, Atmospheric Environment, 35, 1663-1671, 2001.

Kirchstetter, T. W., Novakov, T., and Hobbs, P. V.: Evidence that the spectral dependence of light absorption by aerosols is affected by organic carbon, Journal of Geophysical Research: Atmospheres 109, 2004.

Koistinen, K. J., Kousa, A., Tenhola, V., Hänninen, O., Jantunen, M. J., Oglesby, L., Kuenzli, N., and Georgoulis, L.: Fine particle (PM25) measurement methodology, quality assurance procedures, and pilot results of the EXPOLIS study, J. Air Waste Manage. Assoc., 49, 1212-1220, 1999.

Kubelka, P.: New contributions to the optics of intensely light-scattering materials. Part I, Josa, 38, 448-457, 1948.

Lack, D. A., Cappa, C. D., Covert, D. S., Baynard, T., Massoli, P., Sierau, B., Bates, T. S., Quinn, P. K., Lovejoy, E. R., and Ravishankara, A.: Bias in filter-based aerosol light absorption measurements due to organic aerosol loading: Evidence from ambient measurements, Aerosol Science and Technology, 42, 1033-1041, 2008.

Laskin, A., Laskin, J., and Nizkorodov, S. A.: Chemistry of Atmospheric Brown Carbon, Chemical reviews, 115, 4335-4382, 2015.

Martins, J. V., Artaxo, P., Kaufman, Y. J., Castanho, A. D., and Remer, L. A.: Spectral absorption properties of aerosol particles from 350–2500nm, Geophysical Research Letters, 36, 2009.

5   Martins, J. V., Artaxo, P., Liousse, C., Reid, J. S., Hobbs, P. V., and Kaufman, Y. J.: Effects of black carbon content, particle size, and mixing on light absorption by aerosols from biomass burning in Brazil, J. Geophys. Res.: Atmos., 103, 32041-32050, 1998.

Moosmüller, H., Chakrabarty, R., and Arnott, W.: Aerosol light absorption and its measurement: A review, Journal of Quantitative Spectroscopy and Radiative Transfer, 110, 844-878, 2009.

10   Pandey, A., Pervez, S., and Chakrabarty, R. K.: Filter-based measurements of UV–vis mass absorption cross sections of organic carbon aerosol from residential biomass combustion: Preliminary findings and sources of uncertainty, J. Quant. Spectrosc. Radiat. Transfer, 182, 296-304, 2016.

Petzold, A. and Schönlinner, M.: Multi-angle absorption photometry—a new method for the measurement of aerosol light absorption and atmospheric black carbon, Journal of Aerosol Science, 35, 421-441, 2004.

15   Ramanathan, V., Crutzen, P., Kiehl, J., and Rosenfeld, D.: Aerosols, climate, and the hydrological cycle, Science, 294, 2119-2124, 2001.

Reid, J. S., Eck, T. F., Christopher, S. A., Koppmann, R., Dubovik, O., Eleuterio, D., Holben, B. N., Reid, E. A., and Zhang, J.: A review of biomass burning emissions part III: intensive optical properties of biomass burning particles, Atmos. Chem. Phys., 5, 827-849, 2005.

20   Sagan, C. and Pollack, J. B.: Anisotropic nonconservative scattering and the clouds of Venus, Journal of Geophysical Research, 72, 469-477, 1967.

Schnaiter, M., Schmid, O., Petzold, A., Fritzsche, L., Klein, K.-F., Andreae, M. O., Helas, G., Thielmann, A., Gimmler, M., and Möhler, O.: Measurement of wavelength-resolved light absorption by aerosols utilizing a UV-VIS extinction cell, Aerosol Sci. Technol., 39, 249-260, 2005.

25   Sheridan, P. J., Arnott, W. P., Ogren, J. A., Andrews, E., Atkinson, D. B., Covert, D. S., Moosmüller, H., Petzold, A., Schmid, B., and Strawa, A. W.: The Reno Aerosol Optics Study: An evaluation of aerosol absorption measurement methods, Aerosol Sci. Technol., 39, 1-16, 2005.

Snider, G., Weagle, C., Martin, R., Van Donkelaar, A., Conrad, K., Cunningham, D., Gordon, C., Zwicker, M., Akoshile, C., and Artaxo, P.: SPARTAN: a global network to evaluate and enhance satellite-based estimates of ground-level particulate

30   matter for global health applications, Atmos. Meas. Tech., 8, 505, 2015.

Solomon, P. A., Crumpler, D., Flanagan, J. B., Jayanty, R., Rickman, E. E., and McDade, C. E.: US National PM2. 5 chemical speciation monitoring networks—CSN and IMPROVE: description of networks, J. Air Waste Manage. Assoc., 64, 1410-1438, 2014.

Sumlin, B. J., Heinson, Y. W., Shetty, N., Pandey, A., Pattison, R. S., Baker, S., Hao, W. M., and Chakrabarty, R. K.: UV–

35   Vis–IR spectral complex refractive indices and optical properties of brown carbon aerosol from biomass burning, J. Quant. Spectrosc. Radiat. Transfer, 206, 392-398, 2018.

Sumlin, B. J., Pandey, A., Walker, M. J., Pattison, R. S., Williams, B. J., and Chakrabarty, R. K.: Atmospheric Photooxidation Diminishes Light Absorption by Primary Brown Carbon Aerosol from Biomass Burning, Environ Sci Technol Lett, 4, 540-545, 2017.

40   Sun, H., Biedermann, L., and Bond, T. C.: Color of brown carbon: A model for ultraviolet and visible light absorption by organic carbon aerosol, Geophysical research letters, 34, 2007.

Vecchi, R., Bernardoni, V., Paganelli, C., and Valli, G.: A filter-based light-absorption measurement with polar photometer: Effects of sampling artifacts from organic carbon, J. Aerosol Sci., 70, 15-25, 2014.

Virkkula, A.: Correction of the calibration of the 3-wavelength Particle Soot Absorption Photometer (3λ PSAP), Aerosol Sci.

45   Technol., 44, 706-712, 2010.

Virkkula, A., Ahlquist, N. C., Covert, D. S., Arnott, W. P., Sheridan, P. J., Quinn, P. K., and Coffman, D. J.: Modification, calibration and a field test of an instrument for measuring light absorption by particles, Aerosol Sci. Technol., 39, 68-83, 2005.

Weingartner, E., Saathoff, H., Schnaiter, M., Streit, N., Bitnar, B., and Baltensperger, U.: Absorption of light by soot particles: determination of the absorption coefficient by means of aethalometers, Journal of Aerosol Science, 34, 1445-1463, 2003.

White, W. H., Trzepla, K., Hyslop, N. P., and Schichtel, B. A.: A critical review of filter transmittance measurements for aerosol light absorption, and de novo calibration for a decade of monitoring on PTFE membranes, Aerosol Science and Technology, 50, 984-1002, 2016.

Zhong, M. and Jang, M.: Light absorption coefficient measurement of SOA using a UV–Visible spectrometer connected with an integrating sphere, Atmospheric Environment, 45, 4263-4271, 2011.

Table 1: Number of burns conducted, and filter samples collected for each fuel type and combustion phase in this study. Intrinsic optical properties of emissions from each study condition are also given.

Fuel	Combustion phase	SSA			AÅE	Number of burns	Number of filter samples
		375 nm	405 nm	532 nm	375-532 nm		
Dung	smoldering	0.86	0.95	0.98	6.1-6.6	6	7
Peat	smoldering	0.92	0.97	0.99	4.8-6.8	2	3
Sage	smoldering	0.75-0.87	0.86-0.93	0.93-0.97	2.8-5.3	4	14
	mixed	0.56-0.77	0.69-0.84	0.71-0.87	1.5-2.3	3	7
	flaming	0.43-0.65	0.62-0.69	0.69-0.77	0.9-1.4	2	5
Grass	smoldering	0.74	0.87	0.94	3.2-4.7	3	7
	flaming	0.76	0.81	0.85	1.7	1	3
Lodgepole pine	smoldering	0.84	0.93	0.97	4.2	2	3
Ponderosa pine	mixed	0.61-0.84	0.74-0.91	0.76-0.95	1.2-3.0	4	9
	flaming	0.56	0.65	0.65	0.7	1	2
Douglas fir	mixed	0.82	0.89	0.93	2.7	1	2
	flaming	0.60	0.70	0.71	0.9	1	3
Hardwood pellets	mixed	0.80-0.87	0.92-0.95	0.95-0.98	4.1-6.1	1	3
Kerosene	flaming	0.27	0.30	0.31	0.7-1.1	3	7
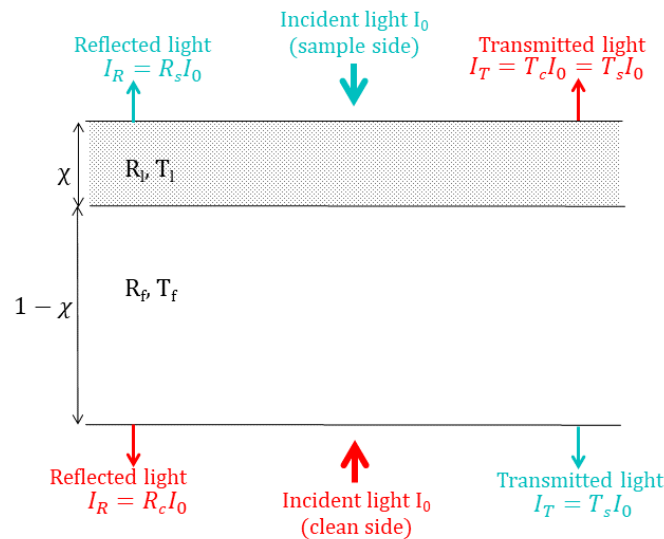
Figure 1: Two-layer model of a filter sample consisting of an aerosol laden layer 'l' and a clean layer 'f'.
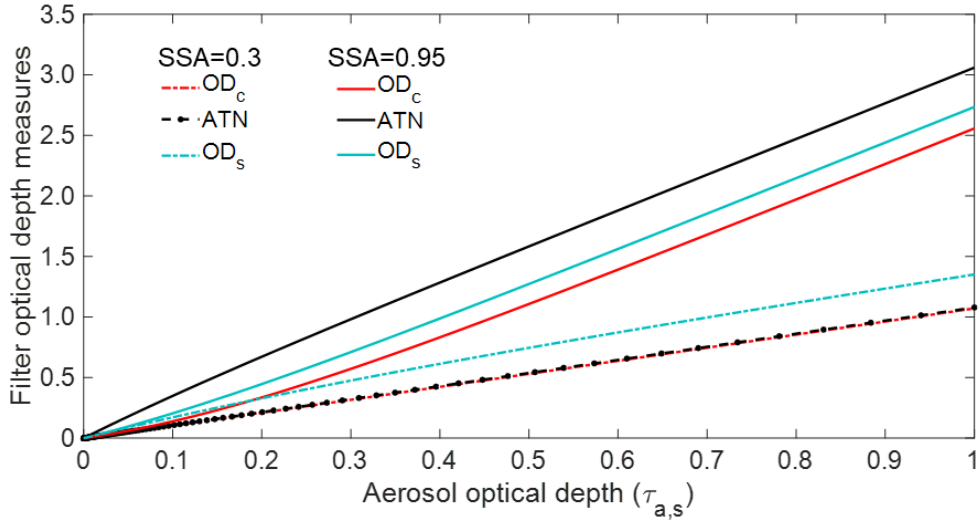
Figure 2: Modeled values of filter optical depth measures (OD_c, ATN and OD_s) with increasing aerosol optical depth ($\tau_{a,s}$) of deposited highly absorbing (SSA=0.3) or highly scattering (SSA=0.95) aerosols. Fixed blank optics were assumed.
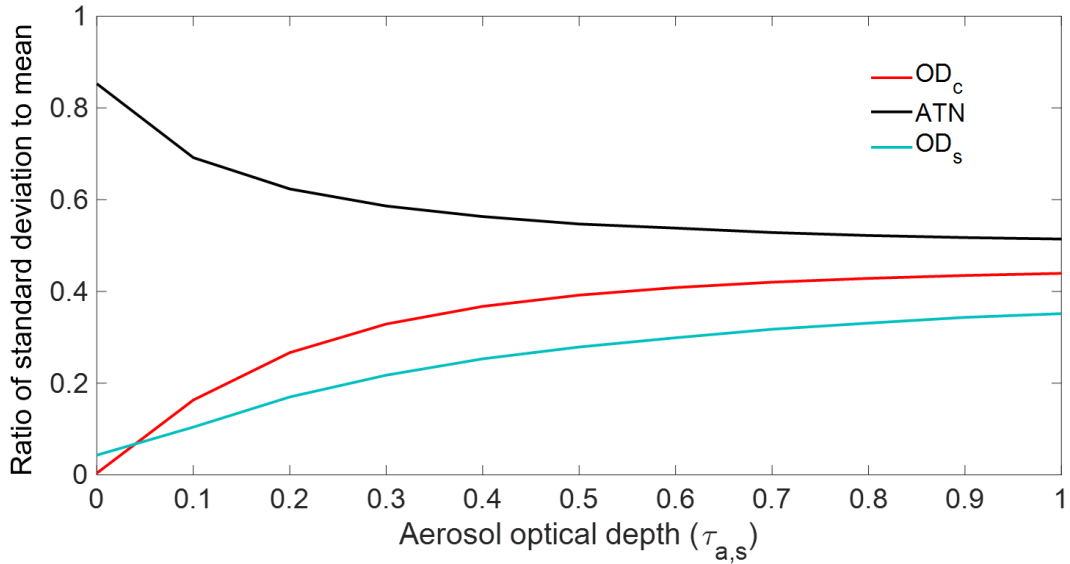
Figure 3: Ratio of standard deviations to means of modeled filter optical depth measures (OD_c, ATN and OD_s) averaged over 500 equally spaced SSA values ranging 0.2-0.99, corresponding to each value of aerosol optical depth ($\tau_{a,s}$). Blank optics were randomly generated for each sample point from a normal distribution with mean=0.7 and standard deviation=0.02.
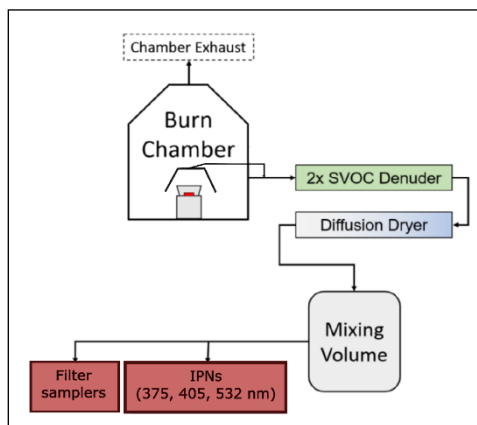
Figure 4: Schematic representation of the experimental setup. Inlet to the semi-volatile organic compound denuder was taken from either the chamber sampling port or the hood. IPN stands for integrated photoacoustic-nephelometer spectrometers.
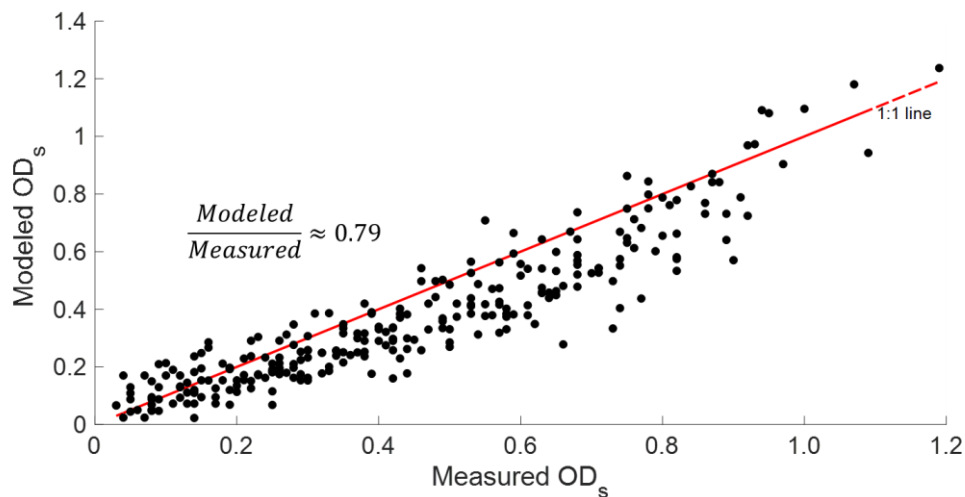
Figure 5: Modeled filter optical depth (OD_s) for absorption optical depth and single scattering albedo values of the aerosols sampled in this study compared with the corresponding filter measurements. A 1:1 line is shown in red. The average ratio of modeled to measured OD_s is 0.79.
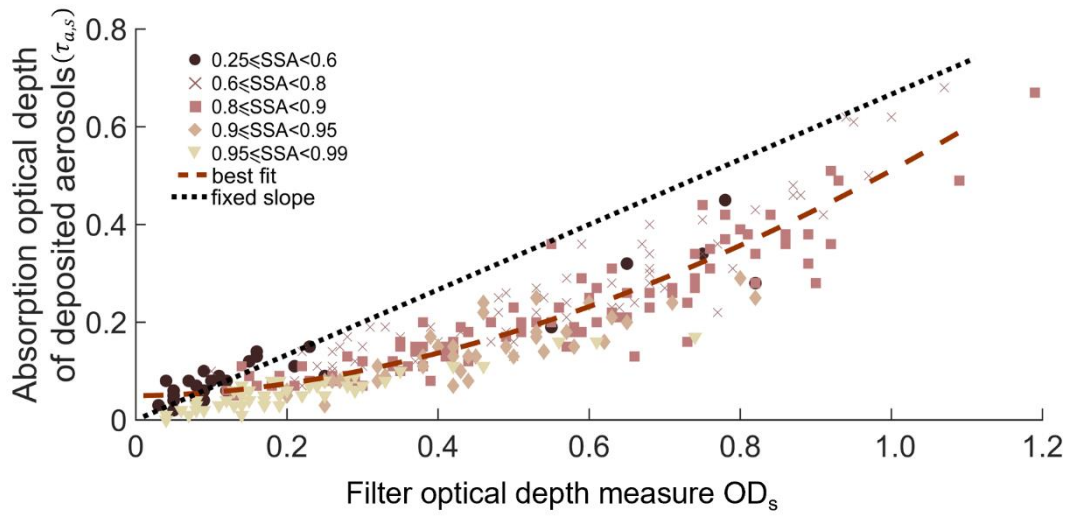
Figure 6: Relationship between *in-situ* aerosol optical depth ($\tau_{a,s}$) and filter optical depth *OD$_s$* through for all (n=75) samples, measured at 375, 405 and 532 nm (N=225 data points). The best fit curve is given by Eq. (10), with R^2 = 0.87. The black perforated line has a fixed slope of 0.67 per (Zhong and Jang, 2011). Uncertainties (1 standard deviation) in *OD$_s$* ranged 2-5%, while those in $\tau_{a,s}$ were 5-10%.
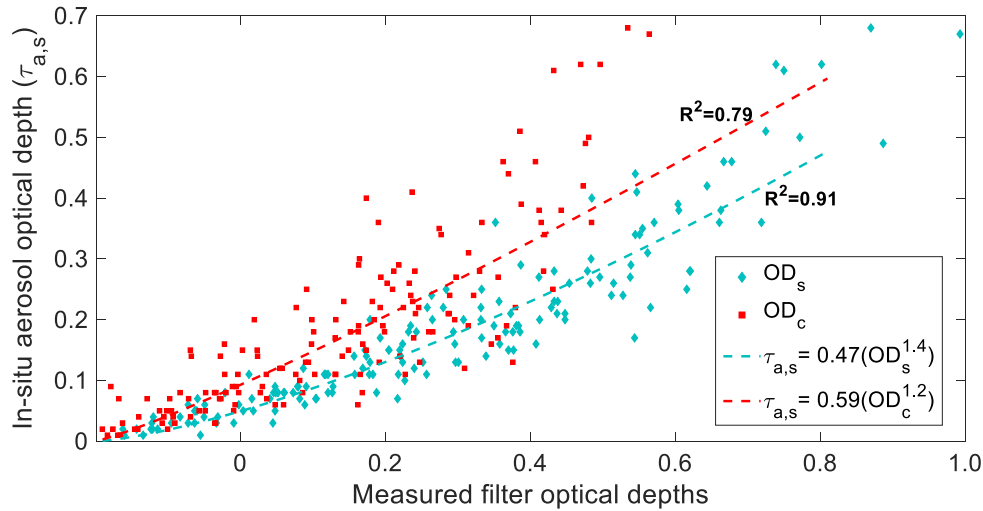
Figure 7: relationship between *in-situ* aerosol optical depth ($\tau_{a,s}$) and measured values of filter optical depth measures *OD$_c$* and *OD$_s$* for a subset of 54 filter samples, measured at 375, 405 and 532 nm (N=162 data points). Uncertainties were as in Fig. 6.
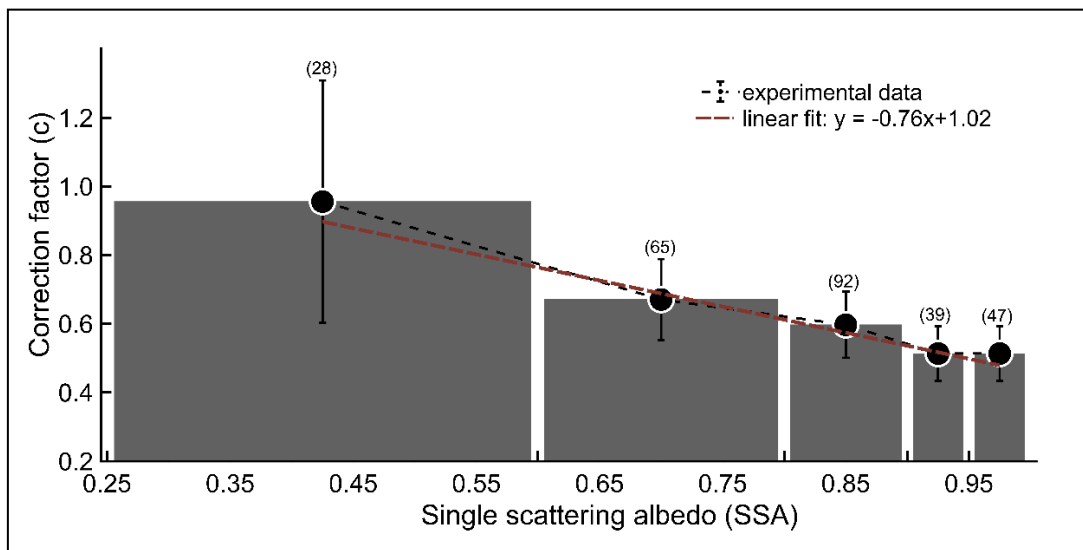
Figure 8: Correction factor C for filter artifacts as a function of single scattering albedo of the deposited aerosols. Error bars show one standard deviation around the mean. The numbers in parentheses denote the number of data points in each bin.